Encapsulating paclitaxel in polymeric nanomicelles increases antitumor activity and prevents peripheral neuropathy

Caroline Mari Ramos Oda [a], Juliana de Oliveira Silva [a], Renata Salgado Fernandes [a], Alysson Vinícius Braga [a], Renes de Resende Machado [a], Márcio de Matos Coelho [a], Geovanni Dantas Cassali [b], Diego Carlos Reis [b], André Luís Branco de Barros [c], Elaine Amaral Leite [a],*

[a] *Department of Pharmaceutical Products, Faculty of Pharmacy, Universidade Federal de Minas Gerais, Av. Antônio Carlos, 6627, 31270-901, Belo Horizonte, Minas Gerais, Brazil*

[b] *Department of General Pathology, Biological Science Institute, Universidade Federal de Minas Gerais, Av. Antônio Carlos, 6627, 31270-901, Belo Horizonte, Minas Gerais, Brazil*

[c] *Department of Clinical and Toxicological Analyses, Faculty of Pharmacy, Universidade Federal de Minas Gerais, Av. Antônio Carlos, 6627, 31270-901, Belo Horizonte, Minas Gerais, Brazil*

ARTICLE INFO

ABSTRACT

Paclitaxel (PTX) has a great clinical significance as an antitumor drug, although several side effects are strongly dose-limiting. In this way, we prepared a PTX-loaded 1,2-distearoyl-sn-glycero-3-phosphoethanolamine-N-[methoxy (polyethylene glycol)-2000] polymeric micelles (PM/PTX) in an attempt to improve safety and effectiveness of conventional PTX formulation (CrEL/EtOH/PTX). In this study, we evaluated from both formulations: stability after dilution, hemocompatibility, cellular uptake, acute toxicity in healthy mice, antitumor activity, and toxicity after multiple-dose treatment. PM/PTX appeared to be more stable than CrEL/EtOH/PTX after dilution. PM/PTX did not exhibit hemolytic activity (values <1%), even at high concentrations. *In vitro* cellular uptake study indicated that polymeric micelles were able to deliver more PTX (5.8 %) than CrEL/EtOH (2.7 %) to 4T1 cells. In the acute toxicity evaluation in healthy mice, CrEL/EtOH/PTX (single dose of 20 mg/kg) induced peripheral neuropathy, which was not observed in PM/PTX group. Similar results were observed after tumor-bearing mice received a multiple-dose regimen (seven doses of 10 mg/kg). Worth mentioning, we also evaluated vehicles, and CrEL/EtOH alone was not capable of inducing neuropathic pain. Besides, PM/PTX exhibited a higher antitumor activity with an inhibition ratio approximately 1.5-fold higher than CrEL/EtOH/PTX group. This study suggested that PM/PTX is safer than CrEL/EtOH/PTX, and was able to improve the antitumor effectiveness in a 4T1 breast cancer model.

1. Introduction

Paclitaxel (PTX) is a chemotherapeutic agent with proven effectiveness for the treatment of metastatic and non-metastatic breast cancer, ovarian cancer, non-small cell lung cancer, prostate cancer, melanoma, esophageal cancer, and other types of solid tumors [1]. However, this drug has poor aqueous solubility, low bioavailability and is often associated with dose-limiting toxicities, such as nephrotoxicity and peripheral neuropathy (PN) [2,3]. The first commercial product named Taxol® was approved by the Food and Drug Administration (FDA) for clinical use in ovarian cancer in 1992. This product and its generic versions are micellar formulations prepared with ethanol and Cremophor EL (CrEL), a synthetic and nonionic surfactant [4]. Even though CrEL has been used as a vehicle for PTX, it is associated with severe and sometimes fatal anaphylactic reactions, and pre-treatment with corticosteroids and antihistamines is commonly required [5,6].

In recent years, pharmaceutical companies have heavily invested in alternatives to carrier PTX [2]. In search of new PTX formulations, nanoparticle albumin-bound PTX (nab-PTX), called Abraxane®, emerged with advantages over Taxol®, such as higher maximum tolerated dose, and it has been taking much of the PTX market [7,8]. However, the therapy with Abraxane® is also associated with a high

---

incidence of PN, which is dose-limiting, painful, and cumulative, often interfering with the continuity of PTX treatment [9].

Therefore, the development of new and advantageous PTX formulations is of great clinical and economic interest. At this time, there are at least 18 companies focused on the pre-clinical or clinical development of nanoformulations of this drug [10]. These PTX-nanocarriers may favor a higher antitumor efficacy with fewer side effects due to a remarkable enhanced permeability and retention (EPR) effect [11]. Among the studied nanosystems, polymeric micelles (PM) have shown as a promising tool for cancer therapy. These nanostructures with size ranging from 5 to 100 nm are formed by block or graft copolymers with a biphasic composition, consisting of an inner hydrophobic core and an outer hydrophilic shell [12]. Structural characteristics of PM can provide important pharmacodynamic and pharmacokinetic advantages, which lead to an increased blood circulation time, a passive targeting in the tumor region, and/or a sustained release of the drug, properties that bypass free PTX drawbacks [13]. PM made up of 1,2-distearoyl-sn-glycero-3-phosphoethanolamine-*N*-methoxy (polyethylen eglycol)-2000] (DSPE-PEG$_{2000}$) are one of the most studied micelles worldwide due to their biocompatibility, biodegradability, and other advantageous properties [14–16]. Our research group has recently developed a kit formulation of PM composed of DSPE-PEG$_{2000}$ containing PTX. This formulation showed tumor targeting and enabled the theranostic use in a solid tumor by ^{99m}Tc-radiolabeling [17]. At this moment, the *in vivo* effectiveness and the ability of this system to reduce PTX side effects remain to be investigated. Thus, in this study, we aimed to examine the ability of PTX-loaded PM to treat a murine breast tumor model. Furthermore, toxicity was investigated by evaluating and comparing hemolysis, acute histopathological changes, and PN induced by PTX-loaded PM and conventional formulation.

2. Material and methods

2.1. Material

1,2-distearoyl-sn-glycero-3-phosphoethanolamine-N-[methoxy (polyethylene glycol)-2000] (DSPE-mPEG$_{2000}$) was acquired from Lipoid GmbH (Ludwigshafen, Germany). PTX with purity greater than 97 % was supplied by Quiral Química do Brasil S/A (Juiz de Fora, Brazil). Cremophor® EL was acquired from Sigma-Aldrich Co (Missouri, USA). Ultra-pure water was obtained using Milli-Q® distillation and deionization equipment (Millipore, USA). Technetium–99 m was obtained from an alumina-based ^{99}Mo/^{99m}Tc generator from the Institute of Energy and Nuclear Research (IPEN, São Paulo, Brazil). All other reagents were acquired from Sigma-Aldrich Co (Missouri, USA).

Murine mammary carcinoma cell line (4T1) was purchased from the American Type Culture Collection (Rockville, USA). Female BALB/c and Swiss mice were purchased from the Bioterism Center of Federal University of Minas Gerais (CEBIO-UFMG) and Faculty of Pharmacy of the UFMG, respectively. All mice were 6–8 weeks old and weighed 20 ± 2 g. The mice were housed in cages in a controlled environment with a temperature set at 25 ± 2 °C, humidity range of 30–70 %, a 12 h light-dark cycle, and free access to food and water. *In vivo* studies were conducted under the approval of the local Ethics Committee on Animal Use (CEUA) following the National Institutes of Health Guide for the Care and Use of Laboratory Animals.

2.2. Paclitaxel dispersion preparation

A micellar dispersion of PTX (CrEL/EtOH/PTX) was prepared by dissolving 30.0 mg of the drug in 5.0 mL of a mixture of CrEL™:dehydrated ethanol (1:1 v/v) under vigorous stirring. Before intravenous injection, this dispersion was diluted in NaCl 0.9 % (w/v) solution at a concentration of 0.6 mg/mL.

2.3. Preparation of PM

PM formulations were prepared using a solvent evaporation method [18,19]. For DTPA-functionalized PM, DSPE-PEG$_{2000}$-DTPA was synthesized according to the method described previously [20]. Chloroformic solutions of DSPE-mPEG$_{2000}$ and DSPE-PEG$_{2000}$-DTPA 99:1 (w/w), respectively (10 mmol/L final concentration), and PTX (0.6 mg/mL) were transferred to a round bottom flask. The solvent was completely removed under reduced pressure. The thin film formed was hydrated with NaCl 0.9 % (w/v), in a water bath at 40 °C for 5 min, followed by vortexing at 1500 g for 3 min. Then, the formulations were transferred to amber and cryo-resistant vials containing glucose as a cryoprotectant in a sugar:polymer ratio of 2:1 (w/w). Vials were frozen in liquid nitrogen and lyophilized in a 24-h cycle using a Modulyo lyophilizer (Thermo Electron Corporation, USA). After the lyophilization cycle, vials were sealed under vacuum, stored sheltered from the light and kept at −20 °C.

At the time of use, the freeze-dried PM was reconstituted by adding ultra-pure water, and after 15 min, the preparation was filtered in 0.22 μm polycarbonate membranes to remove non-encapsulated PTX.

2.4. Physicochemical characterization

Mean diameter was determined by dynamic light scattering (DLS) and zeta potential was evaluated by DLS associated with electrophoretic mobility. Both were investigated at 25 °C and an angle of 90°, using a Zetasizer NanoZS90 instrument (Malvern Instruments, England). For these analyzes, all the samples were diluted 15-fold in NaCl 0.9 % (w/v) solution previously filtered on a 0.45 μm pore membrane.

The content of PTX encapsulated in the formulation was evaluated by high-performance liquid chromatography (HPLC) using a previously validated analytical method [21].

2.5. Formulations stability after dilution

This study was conducted according to the dilution method proposed by De Barros et al. [22]. An aliquot of 92 μL of the PM/PTX or CrEL/EtOH/PTX was incubated in 1.0 mL of pH 7.4 saline-phosphate buffer (PBS) at 37 °C under stirring at 500 bpm (Dubnoff Metabolic Bath MA-95/CF Marconi, Brazil). After 5, 15, 30, 60, 120, 240, 360, 480, and 1440 min, vials (n = 4) were centrifuged at 24,000 g for 15 min to remove released PTX. The amount of remaining encapsulated PTX present in the supernatant at different times (Q_T), as well as the initial amount of drug encapsulated (Q_0), were determined. PTX in Q_T and Q_0 was extracted from PM/PTX using isopropyl alcohol and quantified in HPLC. The release profile was calculated indirectly by the percentage of PTX retained within micelles over time and calculated using Eq. 1.

$$\text{Released PTX } (\%) = 100 - \left(\frac{QT}{Q0} \times 100\right) \tag{1}$$

2.6. Cellular uptake

Cellular uptake was investigated according to the protocols previously described in the literature [23,24] Briefly, PM-DTPA/PTX and CrEL/EtOH/PTX were radiolabeled with ^{99m}Tc as reported by our group [20,25]. 4T1 cells (1.5×10^6 cells), in the culture medium, were incubated with 0.021 μmol of each ^{99m}Tc-labeled formulation at 37 °C under stirring (Metabolic Bath Dubnoff MA-95/CF Marconi, Brazil). At different times (15, 30, 60, and 120 min) after incubation, the samples were centrifuged at 500 g for 5 min at room temperature. The supernatant was removed, and the pellet was washed with 1.0 mL of PBS to remove the non-uptaken micelles. Then, the radioactivity presented in both (pellet and supernatant, n = 5) was quantified in a gamma counter. The percentage of uptake was calculated by using Eq. 2:

$$Uptake\ (\%) = \frac{radioactivity\ pellet}{radioactivity\ pellet\ +\ radioactivity\ supernatant} x\ 100 \qquad (2)$$

The amount of PTX associated with 4T1 cells was quantified by HPLC. After quantifying the radioactivity, 1.0 mL of acetonitrile was added to the pellet and the preparation was taken to the ultrasonic bath for 5.0 min to lyse the cells and precipitate the protein. The samples were centrifuged at 3100 *g* for 15 min at room temperature, and an aliquot of the supernatant was used for quantifying PTX (PTX sample). The percentage of PTX uptake was calculated by using Eq. 3:

$$Uptake\ of\ PTX\ (\%) = \frac{[PTX]sample}{[PTX]total} x\ 100 \qquad (3)$$

2.7. Hemocompatibility evaluation

The hemolytic potential of PM was assessed according to reported in the literature and compared to CrEL/EtOH formulation [26–28]. Fresh blood was obtained from female Swiss mice (Ethics Committee on Animal Use - CEUA from UFMG, protocol number 148/2017). Blood samples were collected in tubes containing 10 % w/v EDTA solution. The red blood cells (RBC) were separated by centrifugation at 1100 *g* for 10 min at room temperature (Heraeus Multifage X1R Centrifuge, Germany). RBC collected from the bottom were washed with NaCl 0.9 % (w/v) until a colorless supernatant was obtained. The final pellet was diluted with NaCl 0.9 % (w/v) solution to obtain a 2% (w/v) RBC concentration. The formulations evaluated were MP/PTX and CrEL/EtOH/PTX at concentrations of 0.05 and 0.1 mg/mL, and their respective controls. The samples were added to 500 μL of 2% RBC suspension (n = 5), the volume was completed to 1 mL with NaCl 0.9 % (w/v), and then, the samples were incubated for 1 h at 37 °C under agitation at 500 bpm (Metabolic Bath Dubnoff MA-95/CF Marconi, Brazil). After the incubation time, the cell suspensions were centrifuged at 500 *g* for 5 min and the amount of hemoglobin released to the supernatant absorbance was measured in a spectrophotometer (Evolution 201 UV–vis Spectrophotometer Thermo Scientific, USA) at 540 nm. NaCl 0.9 % (w/v) was used as a negative control (NC), while ultra-pure water was used as a positive (PC) control. The percent hemolysis was calculated by using Eq. 4:

$$Hemolysis\ (\%) = \frac{Sample\ Absorbance\ -\ NC\ Absorbance}{PC\ Absorbance\ -\ NC\ Absorbance} x\ 100 \qquad (4)$$

2.8. Acute toxicity

A single dose of PM/PTX or CrEL/EtOH/PTX (20 mg/kg) was intravenously administrated into healthy BALB/c mice (n = 6). After treatments, the animals were observed for 14 days and behavioral/clinical modifications, body weight, morbidity, and mortality were evaluated (OECD Guideline for Testing of Chemicals, 2001). After this time, the mice were anesthetized with a mixture of ketamine (80 mg/kg) and xylazine (15 mg/kg), and blood was collected by puncture of the brachial plexus in tubes containing 10 % w/v EDTA solution (Ethics Committee on Animal Use - CEUA from UFMG, protocol number 310/2017). Hematological parameters such as hemoglobin (HGB), number of red blood cells (RBC), hematocrit (HTC), platelets (PLT) total white blood cells (WBC), granulocytes and non-granulocytes were evaluated for each group. For biochemical analysis, blood was centrifuged (1100 *g*, 15 min) and the plasma obtained was frozen at −70 °C. The tests were performed in the Bioplus BIO-2000 semiautomatic analyzer (São Paulo, Brazil) using commercial kits (Labtest, Lagoa Santa, Brazil). Renal function was evaluated by the measurement of urea and creatinine; liver function by determination of alanine aminotransferase (ALT) and aspartate aminotransferase (AST) activity.

After collecting the blood, the mice were euthanized, and the liver, spleen, and kidneys were removed for histopathological evaluation. Organs were set in 10 % (v/v) buffered formalin, embedded in paraffin blocks, and a 4-μm thickness tissue was placed onto glass slides and stained with hematoxylin-eosin. Images of cross-sections were obtained for evaluation using a micro camera (Spot Insight Color, SPOT Imaging Solutions, Sterling Heights, Michigan, USA) attached to a microscope (Olympus BX-40, Olympus, Tokyo, Japan). SPOT software (version 3.4.5) was used for image analysis.

2.9. Peripheral neuropathy evaluation

PTX peripheral neurotoxicity was evaluated by measuring the paw withdrawal threshold (PWT) according to a model previously described [29]. PWT was evaluated at the right hind paw of female BALB/c mice using an electronic von Frey apparatus (Model EFF 301, Insight, Brazil). Initially, the mice were acclimatized at the experimental apparatus for 1 h per day for 2 days, and the basal PWT of each animal was determined (mean of three measurements). Afterward, PM/PTX or CrEL/EtOH/PTX (20 mg/kg) was administered by the tail vein of mice (n = 6) and PWT was evaluated every 2 days during 14 days after administration.

2.10. Antitumor activity

Aliquots of 100 μL containing 5×10^6 4T1 cells in RPMI were injected subcutaneously into the right flank of female BALB/c mice (6-weeks old, 20.0 ± 2.0 g). Tumor cells were allowed to grow for 7 days. When the tumor volume reached approximately 100 mm³, animals were randomly divided into five experimental groups, six animals per group (saline 0.9 % (w/w); CrEL/EtOH, CrEL/EtOH/PTX, blank PM and PM/PTX). Each treated animal received a cumulative dose of 70 mg/kg split into seven administrations, or correspondent volume (control group), *via* the tail vein, each other day. The first day of treatment was considered day zero (D0) of the study. Antitumor activity was evaluated over 16 days and was based on the tumor volume and the tumor growth inhibition ratio determination, tumor-to-muscle ratio using the ^{99m}Tc-radiolabeled polymeric micelles, and immunohistochemical of the tumor tissue. This study was approved by the Ethics Committee on Animal Use from UFMG with protocol number 205/2013.

The tumor volume (V) was evaluated twice a week by the measurements of two orthogonal diameters (d1 and d2) with a slide caliper (Mitutoyo, MIP/E-103), where d1 and d2 were the smallest and the largest perpendicular diameters, respectively, and it was calculated as follows: $v = d1^2 x\ d2 \times 0.5$ [27]. Tumor growth was monitored before the treatment (D0) and the administration of each dose. Mice body weight was also monitored at the same time. At the end of the experimental period (D16), the relative tumor volume (RTV) and the inhibition ratio (IR) for each experimental group were determined by using Eqs. 5 and 6, respectively.

$$RTV = \frac{Tumor\ volume\ on\ D16}{Tumor\ volume\ on\ D0} \qquad (5)$$

$$IR\ (\%) = \frac{mean\ RTV\ from\ each\ treatment}{mean\ RTV\ from\ control\ group} x\ 100 \qquad (6)$$

Ex vivo tumor-to-muscle ratio was also determined to evaluate viable tissue in the tumoral area. For this, at D16 mice received, intravenously, 37 MBq of ^{99m}Tc-DTPA-PM. At 4 h post-administration, mice were anesthetized with a mixture of ketamine (80 mg/kg) and xylazine (15 mg/kg) and euthanized. After euthanasia, muscle of contralateral flank and tumor were collected, weighed, and taken to an automatic scintillation apparatus to determine the radioactivity. Results were expressed as the percentage of injected dose per gram (%ID/g) of tissue.

2.10.1. Immunohistochemistry

After quantifying the radioactivity, the tumor tissue was fixed in formalin (10 % w/v in phosphate-buffered saline, pH 7.4) and embedded in paraffin blocks. Sections with 4 μm thickness were placed onto glass slides, and CDC47 and caspase-3 immunolabeling were performed in tumor sections subjected to heat-induced antigen retrieval in a

water bath with citrate buffer pH 6 (DakoCytomation, Carpinteria, CA, USA) at 98 °C for 20 min. Endogenous peroxidase activity was blocked with 3% hydrogen peroxidase in methanol. Slides were then washed and incubated with primary antibodies (CDC47, 1:300, clone 47DC141 or caspase-3, polyclonal, both from Neomarkers, Fremont, CA). CDC47 expression index was determined by estimating the percentage of positive cells in 500 tumor cells [30], while caspase-3 expression by counting the number of positive neoplastic cells in 10 fields, thoroughly enclosing the histological section with a 40× objective.

2.11. Treatment toxicity evaluation

It was observed behavioral/clinical modifications, body weight, and peripheral neuropathy during treatment. At the end of treatment, a laboratory investigation was performed (hematological and biochemical) in the blood samples.

2.12. Statistical analysis

Statistical analyses were performed using GraphPad Prism 5.0 software. The normality and homogeneity of the variance analysis were verified by D'Agostino-Pearson's and Bartlett's tests, respectively. The difference among experimental groups was tested using the one-way analysis of variance (ANOVA), followed by the Tukey's test. The hemolytic activity data were transformed as cubic root (variable). Differences were considered significant when p values were lower or equal to 0.05 ($p \leq 0.05$).

3. Results

3.1. Physicochemical characterization

The physicochemical characteristics of PM are presented in Table 1. No significant differences were observed among blank PM, PM/PTX, and PM-DTPA/PTX in mean diameter and zeta potential. Size distribution analysis of all formulations showed that over 99 % of particles presented less than 20 nm, indicating uniformity in the particle size. The encapsulation was about 100 % of drug content (around 0.6 mg/mL) in both formulations containing PTX.

3.2. Stability of PTX in PM after dilution

The amount of PTX released from PM was analyzed to evaluate the stability after dilution in comparison with the CrEL/EtOH/PTX formulation (Fig. 1). The data indicated that PM was able to control drug release overtime. From 30 min, the release of PTX from PM was significantly lower ($p < 0.05$) than CrEL/EtOH/PTX. Besides, after 6h, PM/PTX released around 16 % of the drug, while approximately 66 % was released from the PM. Thus, these data suggest that the studied PM is more stable after dilution than the micellar dispersion for CrEL/EtOH.

3.3. Cellular uptake of DTPA-PM/PTX and CrEL/EtOH/PTX

The results of the cellular uptake of ^{99m}Tc-radiolabeled nanosystems and the drug content are shown in Fig. 2. A higher uptake ($p \leq 0.05$) of ^{99m}Tc-CrEL/EtOH/PTX formulation at incubation times of 15 (2.4 ± 0.6
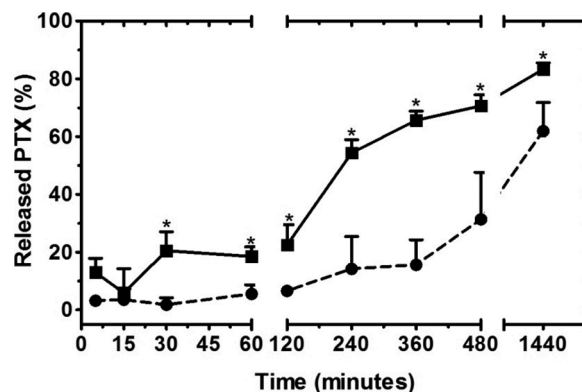
Fig. 1. Evaluation of PTX released from PM/PTX and CrEL/EtOH/PTX formulations overtime after dilution in PBS pH 7.4. Circles and squares represent PM/PTX and CrEL/EtOH/PTX, respectively.
* Represents a significant difference when compared to the PM/PTX at the same time ($p \leq 0.05$). Data were plotted as the mean ± SD (n = 4).
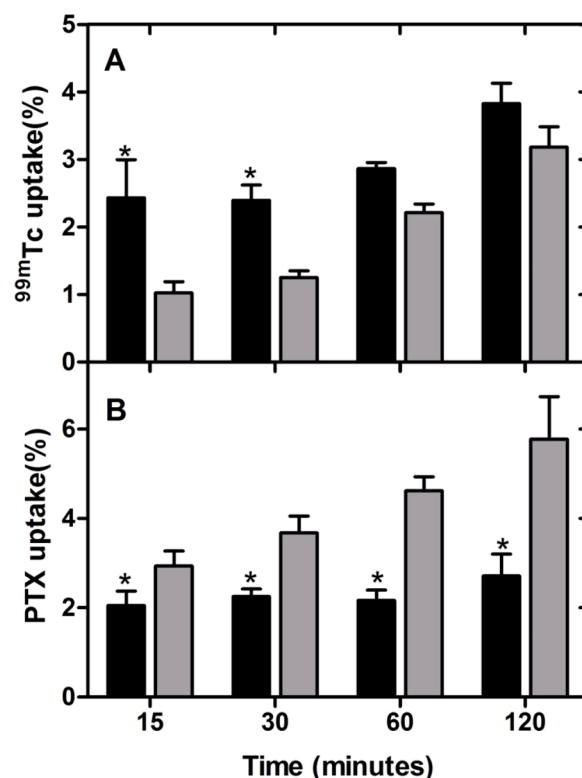
Fig. 2. Cellular uptake studies. (A) Technetium–99 m radiolabeled formulations were incubated with 4T1 tumor cells and the radioactivity quantified in a gamma counter. (B) PTX associated with 4T1 cells and quantified by HPLC. Black and gray bars represent CrEL/EtOH/PTX and PM-DTPA/PTX, respectively.
*Represents a significant difference when compared with PM/PTX in the respective time ($p \leq 0.05$). Data were expressed as the mean ± standard deviation, n = 5.

Table 1
Physicochemical characterization of PM formulations.

Formulations	Mean diameter (nm)	Size distribution	Zeta potential (mV)	PTX content* (%)
Blank PM	10.4 ± 0.3	~99 %, 7 to 18 nm	−2.9 ± 1.3	–
PM/PTX	10.7 ± 0.8	~99 %, 7 to 16 nm	−3.0 ± 0.4	98 ± 5
PM-DTPA/PTX (99:1)	9.5 ± 0.8	~99 %, 6 to 16 nm	−2.4 ± 1.2	99 ± 8

* PTX content is the percentage encapsulated from an initial concentration of 0.6 mg/mL. Data represent the mean ± standard deviation (n = 3).

%) and 30 (2.4 $\pm$ 0.2 %) min when compared to ^{99m}Tc-DTPA-PM/PTX (1.0 $\pm$ 0.2 % and 1.2 $\pm$ 0.1 %, respectively) was observed (Fig. 2A), although no difference between them was found after 60 min. In contrast, a higher amount of PTX ($p \leq 0.05$) in the 4T1 cells was observed for PM/PTX throughout the study (Fig. 2B).

3.4. Hemocompatibility evaluation

Data from hemolytic studies of the PM/PTX and CrEL/EtOH/PTX, as well as the vehicles, are shown in Fig. 3. The results were classified as non-hemolytic (up to 2% hemolysis), moderately hemolytic (above 2% and less than 5%) and hemolytic (more than 5%) as recommended by the International protocol E2524−08 of American Society for Testing and Materials [31].

The comparison of the hemolytic activity in the same concentration showed that PM was significantly (p < 0.05) less hemolytic than CrEL/EtOH, except at the smallest one. CrEL/EtOH/PTX was classified as highly hemolytic (6% and 16 % for 0.05 and 0.10 mg/mL, respectively), and the vehicle at the same dilution showed moderate hemolytic activity (4% of hemolysis) at the concentration of 0.10 mg/mL. On the other hand, incorporating PTX into PM, the hemolysis was remarkably reduced to values lower than 0.5 % in both concentrations. The hemolytic activity observed for blank PM at the same dilution was also less than 0.5 %. Thus, the values obtained for PM containing or not PTX were considered predictive of low toxicity.

3.5. Acute toxicity

Hematological parameters of healthy mice and mice treated with PM/PTX or CrEL/EtOH/PTX are shown in Table 2. RBC and platelets numbers, HGB concentrations, and HCT values were similar in both groups and presented no significant difference (p > 0.05) when compared to those of the control group (healthy mice). In addition, there was no change in the leucocyte series for all groups.

Biochemical parameters indicative of renal (urea and creatinine) and hepatic (ALT and AST) toxicity are also summarized in Table 2. Hepatic parameters did not show significant changes among groups. CrEL/EtOH/PTX group presented a significant increase in the urea levels compared to PM/PTX and control group. The creatinine values in both treated groups were significantly different from the control group. By calculating the index urea/creatinine, the results suggest initial renal
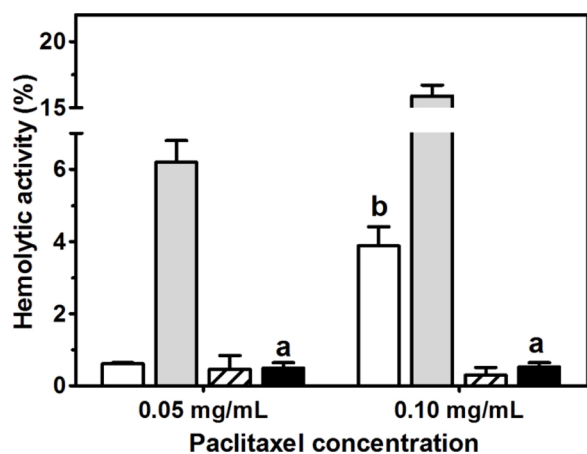
Fig. 3. Hemolysis percentages measured after incubation of red blood cells with PM/PTX (black bars) and CrEL/EtOH/PTX (gray bars) at concentrations of 0.05 and 0.10 mg/mL, and CrEL/EtOH (white bars) and PM (dashed bars). Data were expressed as the mean ± standard error mean, n = 5. * p-value ≤ 0.05. [a]Represents a significant difference when compared to CrEL/EtOH/PTX at the same concentration. [b] Represents a significant difference when compared to CrEL/EtOH/PTX0.1 mg/mL.

Table 2

Hematological and biochemical parameters of healthy mice and mice treated with a single dose of PTX formulations.

Parameters	Healthy mice	CrEL/EtOH/PTX	PM/PTX
RBC (x10^6 /μL)	6.8 ± 0.2	6.4 ± 0.3	6.5 ± 0.3
HGB (g/dL)	13.4 ± 0.5	12.6 ± 0.9	12.4 ± 0.9
HCT (%)	33.4 ± 1.1	32.0 ± 1.9	32.9 ± 1.4
PLT (x10^3 /μL)	396.5 ± 113.8	329.0 ± 63.1	316.8 ± 30.1
WBC (x10^3 /μL)	6.2 ± 1.3	6.6 ± 0.9	5.3 ± 0.7
Granulocytes (x10^3 /μL)	2.3 ± 0.2	2.8 ± 0.4	2.3 ± 0.4
Non-granulocytes (x10^3 /μL)	3.9 ± 1.1	3.7 ± 0.6	3.0 ± 0.4[a]
Urea (mg/dL)	33.4 ± 3.7	51.8 ± 6.0 [a,b]	40.5 ± 4.7
Creatinine (mg/dL)	0.38 ± 0.07	0.22 ± 0.05[b]	0.23 ± 0.04[b]
Blood urea/creatinine	90.8 ± 23.1	247.6 ± 44.8[a,b]	178.3 ± 29.1[b]
ALT (U/L)	42.8 ± 3.8	35.1 ± 3.7	35.8 ± 7.8
AST (U/L)	95.7 ± 23.5	83.8 ± 22.9	87.4 ± 15.5

Evaluation of the hematological and biochemical parameters was carried out 14 days after treatment of mice with the PTX formulations. Results were expressed as the mean ± standard deviation.
[a] Represents a significant difference when compared to PM/PTX group ($p \leq 0.05$).
[b] Represents a significant difference when compared to the healthy mice group ($p \leq 0.05$). Abbreviations: HGB (hemoglobin), RBC (red blood cells), (HTC) hematocrit, PLT (platelets), WBC (total white blood cells), ALT (alanine aminotransferase), and AST (aspartate aminotransferase).

toxicity for the treated groups since it was about 2.7 and 2.0-fold higher than the control group. However, the value obtained for the PM/PTX group was significantly lower than that of CrEL/EtOH/PTX group. Besides, no histological alteration was observed in the renal and hepatic tissue of the mice treated with different formulations containing PTX (Fig. 4)

Concerning the body weight, no significant variation over time was observed in both groups (p > 0.05), as is shown in Fig. 5A. A slight weight loss was observed in CrEL/EtOH/PTX group on the second day after drug administration, but both groups presented a weight gain at the end of the study. Neither mortality nor clinical toxicity signs such as prostration and intense piloerection were observed in both groups.

PN was also evaluated in BALB/c mice after a single dose (20 mg/kg) of PM/PTX and CrEL/EtOH/PTX (Fig. 5B). Mechanical allodynia, characterized by a reduction of PWT, was already established two days after the administration of CrEL/EtOH/PTX and lasted throughout the experimental period of 14 days. By contrast, no significant (p > 0.05) change of PWT was observed in PM/PTX group. These data suggest that PM had a protective effect against the PN induced by PTX.

3.6. Antitumor activity

Antitumor efficacy data evaluated in 4T1 tumor-bearing BALB/c mice after treatment with a total dose of 70 mg/kg of PTX are presented in Fig. 6A. Although we have evaluated control groups for each treatment formulations using empty formulations, no significant difference among them could be observed; thus, only data from the saline group was presented as the control group. Tumor growth data were also evaluated by regression analysis. The best-fit models and the determination coefficients are shown in Table 3. The first-order mathematical model was obtained for all groups; however, the intercept and inclination were significantly different in all groups, suggesting that the tumor growth was altered by treatment. These data are in line with the IR data, which showed that both treatments were able to reduce tumor growth when compared to the control group; however, PM/PTX group presented a higher IR (approximately 1.5-fold) than CrEL/EtOH/PTX (Table 3).

Besides, the *ex-vivo* tumor-to-muscle uptake ratio evaluation also demonstrated the high efficacy of PM/PTX compared to CrEL/EtOH/PTX. As can be seen in Table 3, a significant reduction of the uptake in the tumor area could be observed for the PM/PTX group in comparison
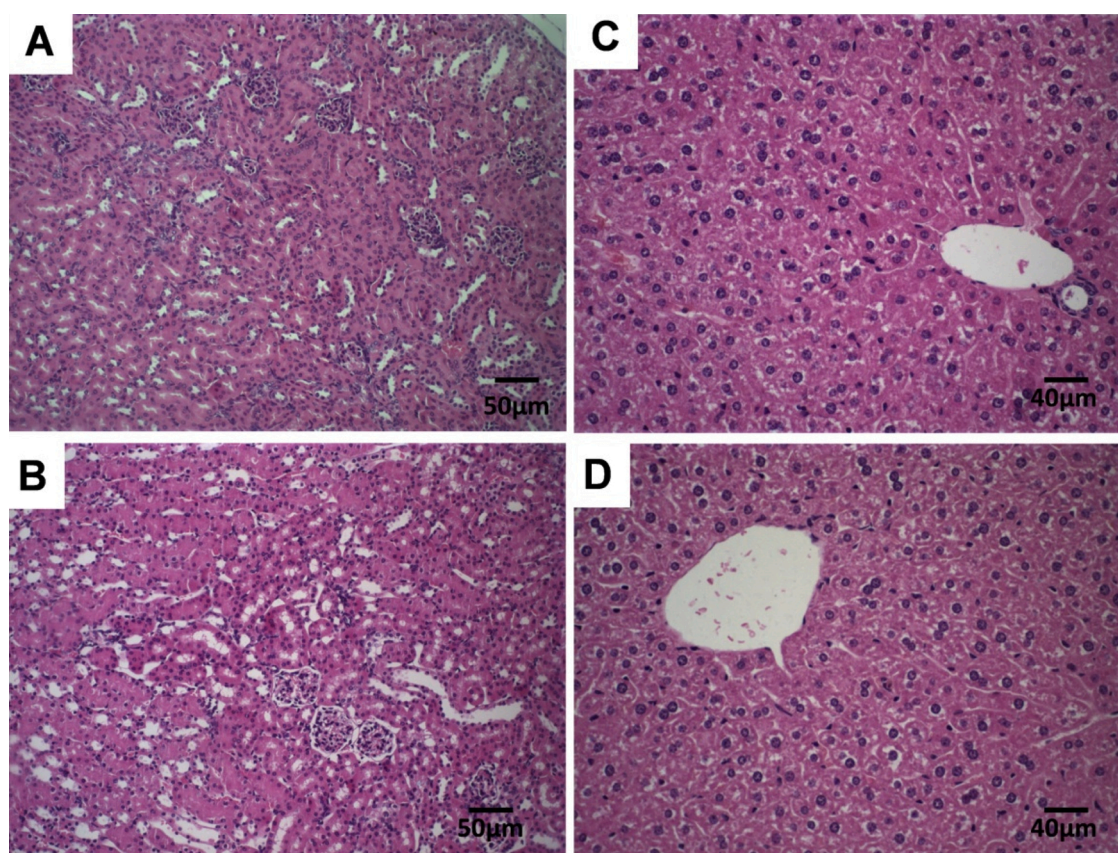
Fig. 4. Photomicrographs of renal (A and B) and hepatic (C and D) tissue from female mice treated with PM/PTX (A and C) and CrEL/EtOH/PTX (B and D). Hematoxylin and eosin.

to CrEL/EtOH/PTX and control groups (p $\leq$ 0.05).

HE histological analysis of tumor tissue presented similar morphological characteristics among groups with central areas of necrosis and proliferation of pleomorphic cells at the periphery infiltrated by leukocytes (data not shown). Thus, we evaluated the levels of CDC-47 and caspase-3 to investigate cellular proliferation and apoptosis in the tumor tissue. The results are presented in Fig. 6B. As observed, the number of positive CDC-47 (around 33 %) cells was significantly lower in PM/PTX group than saline and CrEL/EtOH/PTX groups (44 and 46 %, respectively). About apoptosis-related protein caspase-3, PM/PTX group also demonstrated lower expression compared to CrEL/EtOH/PTX group; however, there was no difference concerning the control group. Representative photographs of the tumors removed from the mice after the treatments can be seen in Fig. 6C. Tumors of the PM/PTX-treated group were noticeably smaller than other groups.

In these experimental groups, we also evaluated the effect of the treatment in the toxicity parameters. Animals of CrEL/EtOH/PTX group presented more stressed than other groups. In addition, CrEL/EtOH/PTX group presented a body weight loss until the 14th day of monitoring, while the other groups showed an initial body weight reduction, nevertheless, no significant difference at the end of the experiment was observed (Fig. 6D). PN induced by repeated doses of PM/PTX and CrEL/EtOH/PTX were also evaluated in tumor-bearing mice. Data presented in Fig. 6E demonstrated that only CrEL/EtOH/PTX sensitized the animals, leading to a significant reduction of the PWT. Formulations vehicles (blank PM and CrEL/EtOH) were also evaluated to verify if they contribute to the sensitization. However, none of them affected mice basal PWT, suggesting that the mechanical allodynia is indeed caused by PTX. Thus, these data reinforce the hypothesis that PM had a protective effect on the PN induced by PTX.

Finally, hematological and biochemical parameters of PM/PTX,

CrEL/EtOH/PTX, and saline groups are shown in Table 4. No significant difference in hematological parameters was observed among groups. However, the comparison of these data with those obtained from healthy mice without treatment (Table 2) demonstrated a substantial increase in WBC (around 6×10^3 cell/μL *versus* 100×10^3 cell/μL). By contrast, no difference was observed in hepatic and renal function parameters ($p > 0.05$).

4. Discussion

PTX is one of the most successful drugs ever used to treat metastatic breast cancer and other solid tumors either as a single agent or associated with other chemotherapeutic drugs [1]. The first marketed product used in clinical therapy with effective antitumor activity was a CrEL-based PTX formulation; however, it has considerable potential for severe toxicity, including hypersensitivity reactions, myelosuppression, and peripheral neuropathy [2]. Drug delivery nanosystems have been widely studied as promising tools to overcome these issues, and increased investments of pharmaceutical and biotech companies are involved [10]. New nanotechnology-based PTX formulations were approved for clinical applications, such as Abraxane™ (PTX albumin-bound nanoparticle) and Genexol-PM™ (polymeric micelles containing PTX) [32]. Enhanced cytotoxic activity against some cancer cells has been reported; however, myelosuppression and sensory neuropathy are still side effects often related to the use of these nanoformulations [33,34]. Thus, the development of formulation with reducing systemic toxicity, hypersensitivity reactions, and capable of accumulating in the tumor region is still a challenge. Our group has already described the lipid-polymer micelles composed of DSPE-PEG2000 to carrier the PTX which showed tumor targeting in a solid tumor model. In order to evaluate whether this finding may
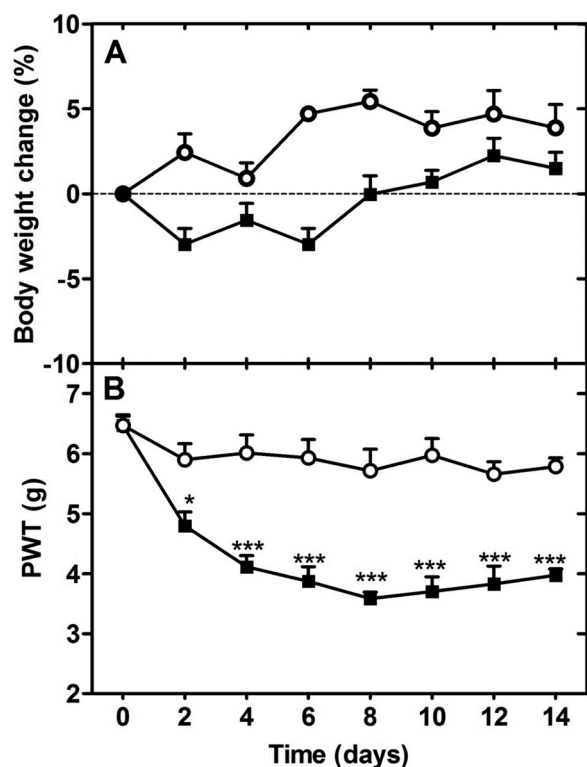
Fig. 5. *In vivo* evaluation of body weight (A) and paw withdrawal threshold (B) changes in healthy BALB/c mice after administration of a single dose (20 mg/kg) of PTX formulations. Circles and squares represent PM/PTX and CrEL/EtOH/PTX, respectively.

Data were expressed as mean ± standard error mean. * and *** Represent a significant difference when compared to PM/PTX group ($p < 0.05$ and $p < 0.001$, respectively), n=7.

improve the therapeutic efficacy of PTX-based treatment, in the present study, we performed *in vitro* and *in vivo* investigations aiming to analyze the advantages of this system to treat tumors as well as to reduce the toxicity compared to a CrEL-based PTX formulation.

The PM/PTX proposed in this study for intravenous administration presented a narrow size distribution of approximately 10 nm and neutral zeta potential. These characteristics are important since they can favor the increase of blood circulation time and lead to accumulation in the tumor tissue by the EPR effect [35,36]. After dilution, PM/PTX exhibited higher stability than CrEL/EtOH/PTX within 24 h. This fact was evidenced at 2 h after dilution since a rapid release of PTX from CrEL/EtOH, around 4-fold higher than PM, was observed. This finding suggests that the PM are suitable as a delivery system, and they are not disrupted after a dilution typically observed after intravenous administration. Additionally, 4T1 uptake studies indicated that PM/PTX delivers a high amount of drug to the cells. Although the nanoparticle uptake pathway cannot be predicted in this study, our data suggest different pathways of cellular internalization for CrEL/EtOH/PTX and PM/PTX, once they present different uptake profiles over time. It is known that some properties of the nanoparticles such as size, zeta potential, and composition are directly related to the cellular uptake mechanism of these systems [37,38]. However, PM presented similar size (10 nm) of CrEL-based micelles as previously described by Monteiro and coworkers [25]. Therefore, probably the composition of the systems was the main parameter that affected the uptake mechanism of each formulation.

Since the intravenous route is the main choice for the administration of PTX due to its low oral absorption [39], we firstly evaluated the potential of the PM/PTX to reduce hemolytic toxicity. It is well-described that after administering pharmaceutical formulations by the intravenous pathway, they unavoidably interact with RBC; thus the hemolytic

activity study can be a good indicator for the toxicity of the developed formulation [31,40]. This study evidenced that PM, containing or not PTX, did not cause lysis of RBC, whereas CrEL/EtOH/PTX was classified as hemolytic at the lower concentration evaluated, suggesting that PM is safer as a PTX carrier than CrEL/EtOH. *In vivo* toxicity studies were also performed in healthy mice after intravenous injection of a high and single dose of PTX, and aggressiveness followed by weakness and inability to move off the mice were observed after CrEL/EtOH/PTX administration. Rabah has already reported similar behavior [41]. By contrast, these effects did not occur in mice treated with PM/PTX. We supposed that this behavior was due to the presence of the CrEL that can cause many side effects, including tachycardia and hypotension [4]. Besides, the biochemical analysis indicated early nephrotoxicity in both treated groups verified by an increase in the urea/creatinine index compared to the control. This index is a good parameter to indicate early renal damage when there is no apparent reduction in the glomerular filtration rate, but there is some tubular damage, reflecting in an alteration only in the urea levels. As kidney injury is a common toxicity of PTX, it is interesting to note that the nephrotoxicity was more pronounced in CrEL/EtOH/PTX group, evidenced by a significant increase in urea levels compared to control and PM/PTX groups [41,42].

As PTX leads to axonal degeneration in peripheral sensory nerves causing PN, which is a dose-limiting side effect, we also evaluated the induction of neuropathic pain by mechanic allodynia after administrating of PTX in different formulations. PN markedly worsens the patient's quality of life due to clinical manifestations such as painful paresthesia or numbness, sensory ataxia, gait disturbance, and weakness [9,43,44]. A reduction and maintenance of the tactile threshold for 14 days were observed for CrEL/EtOH/PTX group (Fig. 6E). These results strongly suggest that PM formulations could prevent CIPN, one of the main side effects of PTX [9].

To verify whether the incorporation of PTX in PM affects the antitumor activity, 4T1 tumor-bearing mice were treated with repeated doses of PTX formulations. Parameters of antitumor activity and toxicity were evaluated. Regarding antitumor activity, PM/PTX were more effective than CrEL/EtOH/PTX formulation in controlling tumor growth. Besides, tumor-to-muscle uptake ratio showed a significant reduction for PM/PTX compared to CrEL/EtOH/PTX, due to the smaller tumor size, again suggesting higher efficacy. In agreement with these results, immunohistochemistry analysis demonstrated a significant reduction of the count of CDC47 positive cells compared to other groups, although there was no difference in the presence of apoptotic cells compared to the control group. As aforementioned, we have already shown that DSPE-PEG PM exhibited the property to accumulate in the tumor site [20]. Thus the set of results allowed us to hypothesize that due to the superior stability after dilution and higher uptake by 4T1 cells, PM were capable of delivering more PTX inside the tumor than CrEL micelles, resulting in higher effectiveness.

Additionally, PM/PTX still showed safer than CrEL/EtOH/PTX even when repeated doses were given. Similarly to observe in the acute toxicity, the mice treated with CrEL/EtOH exhibited more intense distress signs following decreasing body weight were also attributed to the toxic effect of the formulation. Even though the hematological and biochemical parameters of PTX-treated groups did not differ from the saline 0.9 % (w/v) group, especially the WBC count considerably differs from healthy mice (Table 2). These alterations might be attributed to the mammary 4T1 tumor experimental model. Some studies have shown that tumors from the 4T1 cells are associated with an increased level of granulocytes in the bloodstream, characterizing a leukemoid reaction due to the tumor progression [45,46].

Again, effects induced by the formulations on the PWT were evaluated to verify whether empty formulations or the tumor contribute to the mice sensitization. All control groups (saline, CrEL/EtOH, and PM) did not exhibit a PWT decrease, while this effect was observed in the CrEL/EtOH/PTX group, indicating that PTX plays a major role in inducing the mechanical allodynia. On the other hand, the absence of mechanical
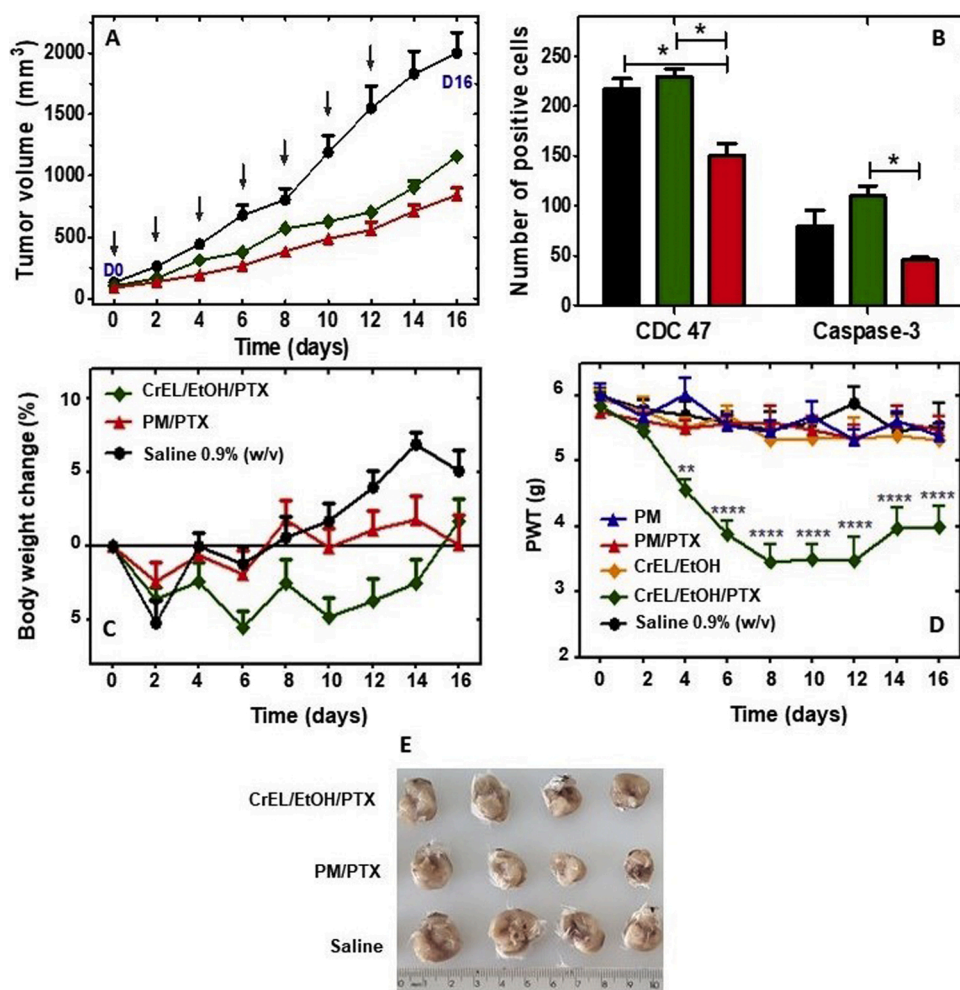
Fig. 6. (A) Tumor volume evaluated after administration of each other day of saline (black), CrEL/EtOH/PTX (green), and PM/PTX (red) at a dose of 10 mg/kg in tumor-bearing BALB/c mice. (B) CDC-47 and caspase-3 positive cells present in the tumor tissue evaluated 16 days after the administration of saline (black), CrEL/EtOH/PTX (green), and PM/PTX (red) in 4T1 tumor-bearing BALB/c mice. (C) Body weight and (D) paw withdrawal threshold changes evaluated after treatment in 4T1 tumor-bearing BALB/c mice. (E) Representative photographs of the tumors after dissection. Arrows in panel A indicate the days of treatment. Data were expressed as mean ± standard error mean (n = 6). * represents significant difference $p < 0.05$; ** ($p < 0.01$) and ***($p < 0.0001$) represent significant difference when compared to other groups at the same time.

Table 3
Parameters of the antitumor evaluation of PTX treatments in 4T1 tumor-bearing BALB/c mice.

Group	Regression model	R^2	RTV	IR (%)	Tumor-to-muscle ratio
Saline 0.9 % (w/v)	Y = 124.8X - 882.4	0.8486	16.3 ± 1.4	–	1.97 ± 0.40
CrEL/EtOH/PTX	Y = 62.26X - 387.7	0.8822	11.7 ± 1.2	29	1.81 ± 0.50
PM/PTX	Y = 45.23X - 264.9	0.9284	9.5 ± 1.3	42	1.05 ± 0.22[a]

Data were expressed as mean ± standard deviation.
[a] Represents a significant difference when compared to other groups ($p < 0.05$). Abbreviations: RTV - Relative Tumor Volume; IR – Inhibition Ratio.

allodynia in the PM/PTX group corroborates the hypothesis that PM, as a carrier for PTX, prevents the PN, the most limiting side effect induced by this chemotherapeutic agent. Despite the advantages reported by using a PTX nanoformulation, such as Abraxane™, this side effect still limits the therapy [10,44,47]. Therefore, PM/PTX showed better performance than CrEL/EtOH that was evidenced by the high effectiveness associated with the complete absence of peripheral neuropathy. These findings could result in a better therapeutic response for antitumor therapy approaches.

5. Conclusion

Our results showed that PM/PTX were more efficacious and less toxic than a conventional formulation. Physically, it proves itself more stable than CrEL/EtOH/PTX after diluting, indicating that PM will not disassemble immediately once in the bloodstream, thus increasing the probability of drug delivery to the tumor site by EPR effect. Due to the

Table 4
Hematological and biochemical parameters of tumor-bearing BALB/c mice treated with cumulative doses of PTX formulations.

Parameters	Saline 0.9 (w/v)	CrEL/EtOH/PTX	PM/PTX
RBC (x10⁶ /μL)	6.5 ± 0.5	5.4 ± 1.0	5.8 ± 0.8
HGB (g/dL)	13.3 ± 1.5	11.3 ± 2.8	12.0 ± 2.2
HCT (%)	31.7 ± 2.8	28.1 ± 5.5	30.1 ± 4.5
PLT (x10³ /μL)	453.0 ± 112.3	363.2 ± 159.1	393.3 ± 158.6
WBC (x10³ /μL)	94.4 ± 26.3	113.5 ± 5.4	106.2 ± 6.2
Granulocytes (x10³ /μL)	85.8 ± 26.3	101.1 ± 15.4	100.5 ± 5.3
Non-granulocytes (x10³ /μL)	8.6 ± 1.9	6.2 ± 0.8	5.8 ± 1.0
Urea (mg/dL)	48.1 ± 8.2	53.5 ± 12.1	45.0 ± 3.0
Creatinine (mg/dL)	0.36 ± 0.05	0.36 ± 0.06	0.32 ± 0.04
ALT (U/L)	36.3 ± 6.4	33.0 ± 7.2	32.5 ± 5.5
AST (U/L)	142.9 ± 11.2	147.3 ± 15.3	178.5 ± 26.7

Data are expressed as mean ± standard deviation.

high stability of PM/PTX, the drug would be less available to induce unspecific effects, reducing the toxicity, particularly the PN. Besides that, PM/PTX exhibited higher antitumor activity than CrEL/EtOH/PTX. In this way, we can infer that this nanocarrier has great potential to be clinically used to reduce well-known dose-limiting toxicity induced by PTX.

Declaration of Competing Interest

The authors report no declarations of interest.

Acknowledgments

References

[1] B.A. Weaver, W. Bement, How Taxol / paclitaxel kills cancer cells, Mol. Biol. Cell 25 (2014) 2677–2681, https://doi.org/10.1091/mbc.E14-04-0916.

[2] E. Bernabeu, M. Cagel, E. Lagomarsino, M. Moretton, D.A. Chiappetta, Paclitaxel : what has been done and the challenges remain ahead, Int. J. Pharm. 526 (2017) 474–495, https://doi.org/10.1016/j.ijpharm.2017.05.016.

[3] R.L. Oostendorp, T. Buckle, G. Lambert, Paclitaxel in self-micro emulsifying formulations : oral bioavailability study in mice, Invest. New Drugs 29 (2011) 768–776, https://doi.org/10.1007/s10637-010-9421-7.

[4] H. Gelderblom, J. Verweij, K. Nooter, A. Sparreboom, E.L. Cremophor, The drawbacks and advantages of vehicle selection for drug formulation, Eur. J. Cancer 37 (2001) 1590–1598, https://doi.org/10.1016/s0959-8049(01)00171-x.

[5] C.-P.H. Yang, S.B. Horwitz, Taxol® : the first microtubule stabilizing agent, Int. J. Mol. Sci. 18 (2017) 11, https://doi.org/10.3390/ijms18081733.

[6] S. Wang, J. Qiu, Z. Shi, Y. Wang, M. Chen, Nanoscale drug delivery for taxanes based on the mechanism of multidrug resistance of cancer, Biotechnol. Adv. 33 (2015) 224–241, https://doi.org/10.1016/j.biotechadv.2014.10.011.

[7] R. De Luca, G. Profita, G. Cicero, Nab-paclitaxel in pretreated metastatic breast cancer : evaluation of activity, safety, and quality of life, Onco. Ther. 12 (2019) 1621–1627, https://doi.org/10.2147/OTT.S191519.

[8] L. Peng, Z. Bu, X. Ye, Y. Zhou, Q. Zhao, Incidence and risk of peripheral neuropathy with nab-paclitaxel in patients with cancer : a meta-analysis, Eur. J. Cancer Care (Engl). 26 (2017) 1–11, https://doi.org/10.1111/ecc.12407.

[9] J. Kamei, S. Hayashi, A. Sakai, Y. Nakanishi, M. Kai, Rikkunshito prevents paclitaxel-induced peripheral neuropathy through the suppression of the nuclear factor kappa B (NF κ B) phosphorylation in spinal cord of mice, PLoS One 12 (2017) e0171819, https://doi.org/10.1371/journal.pone.0171819.

[10] A.M. Sofias, M. Dunne, G. Storm, C. Allen, The battle of "nano" paclitaxel, Adv. Drug Deliv. Rev. 122 (2017) 20–30, https://doi.org/10.1016/j.addr.2017.02.003.

[11] J. Fang, H. Nakamura, H. Maeda, The EPR effect: unique features of tumor blood vessels for drug delivery, factors involved, and limitations and augmentation of the effect, Adv. Drug Deliv. Rev. 63 (2011) 136–151, https://doi.org/10.1016/j.addr.2010.04.009.

[12] K. Kazunori, K. Glenn S, Y. Masayuki, O. Teruo, S. Yasuhisa, Block copolymer micelles as vehicles for drug delivery, J. Control. Release 24 (1993) 119–132, https://doi.org/10.1016/0168-3659(93)90172-2.

[13] C. Oerlemans, W. Bult, M. Bos, G. Storm, J.F.W. Nijsen, W.E. Hennink, Polymeric micelles in anticancer therapy: targeting, imaging and triggered release, Pharm. Res. 27 (2010) 2569–2589, https://doi.org/10.1007/s11095-010-0233-4.

[14] W.-H. Chen, X.-D. Xu, H.-Z. Jia, Q. Lei, G.-F. Luo, S.-X. Cheng, R.-X. Zhuo, X.-Z. Zhang, Therapeutic nanomedicine based on dual-intelligent functionalized gold nanoparticles for cancer imaging and therapy in vivo, Biomaterials. 34 (2013) 8798–8807, https://doi.org/10.1016/j.biomaterials.2013.07.084.

[15] S.R. Croy, G.S. Kwon, Polymeric micelles for drug delivery, Curr. Pharm. Des. 12 (2006) 4669–4684, https://doi.org/10.2174/138161206779026245.

[16] R.D. Dabholkar, R.M. Sawant, D.A. Mongayt, P.V. Devarajan, V.P. Torchilin, Polyethylene glycol-phosphatidylethanolamine conjugate (PEG-PE)-based mixed micelles: some properties, loading with paclitaxel, and modulation of P-glycoprotein-mediated efflux, Int. J. Pharm. 315 (2006) 148–157, https://doi.org/10.1016/j.ijpharm.2006.02.018.

[17] C.M.R. Oda, A.L.B. de Barros, R.S. Fernandes, S.E.M. Miranda, M.X. Teixeira, V.N. Cardoso, M.C. Oliveira, E.A. Leite, Freeze-dried diethylenetriaminepentaacetic acid-functionalized polymeric micelles containing paclitaxel: a kit formulation for theranostic application in cancer, J. Drug Deliv. Sci. Technol. 46 (2018) https://doi.org/10.1016/j.jddst.2018.05.007.

[18] R.R. Sawant, V.P. Torchilin, Multifunctionality of lipid-core micelles for drug delivery and tumour targeting, Mol. Membr. Biol. 27 (2010) 232–246, https://doi.org/10.3109/09687688.2010.516276.

[19] T. Wang, V.A. Petrenko, V.P. Torchilin, Paclitaxel-loaded polymeric micelles modified with MCF-7 cell-specific phage protein: enhanced binding to target

[20] C.M.R. Oda, R.S. Fernandes, S.C.A. Lopes, M.C. de Oliveira, V.N. Cardoso, D.M. Santos, A.M.C. Pimenta, A. Malachias, R. Paniago, D.M. Townsend, P.M. Colletti, D. Rubello, R.J. Alves, A.L.B. de Barros, E.A. Leite, Synthesis, characterization and radiolabeling of polymeric nano-micelles as a platform for tumor delivering, Biomed. Pharmacother. 89 (2017) 268–275, https://doi.org/10.1016/j.biopha.2017.01.144.

[21] M.V. Barbosa, L.O.F. Monteiro, A.R. Malagutti, M.C. Oliveira, A.D. Carvalho-Junior, E.A. Leite, Comparative study of first-derivative spectrophotometry and high performance liquid chromatography methods for quantification of paclitaxel in liposomal formulation, J. Braz. Chem. Soc. 26 (2015) 1338–1343, https://doi.org/10.5935/0103-5053.20150100.

[22] A.L.B. De Barros, L.D.G. Mota, D.C.F. Soares, C.M. De Souza, G.D. Cassali, M.C. Oliveira, V.N. Cardoso, Long-circulating, pH-sensitive liposomes versus long-circulating, non-pH-sensitive liposomes as a delivery system for tumor identification, J. Biomed. Nanotechnol. 9 (2013) 1636–1643, https://doi.org/10.1166/jbn.2013.1649.

[23] S. Nie, W.W. Hsiao, W. Pan, Z. Yang, Thermoreversible Pluronic F127-based hydrogel containing liposomes for the controlled delivery of paclitaxel: in vitro drug release, cell cytotoxicity, and uptake studies, Int. J. Nanomedicine 6 (2011) 151–166, https://doi.org/10.2147/IJN.S15057.

[24] J. Miao, Y. Du, H. Yuan, X. Zhang, F. Hu, Biointerfaces Drug resistance reversal activity of anticancer drug loaded solid lipid nanoparticles in multi-drug resistant cancer cells, Colloids Surf. B Biointerfaces 110 (2013) 74–80, https://doi.org/10.1016/j.colsurfb.2013.03.037.

[25] L.O.F. Monteiro, R.S. Fernandes, L.C. Castro, V.N. Cardoso, M.C. Oliveira, D.M. Townsend, A. Ferretti, D. Rubello, E.A. Leite, A.L.B. De Barros, Technetium-99 m radiolabeled paclitaxel as an imaging probe for breast cancer in vivo, Biomed. Pharmacother. 89 (2017) 146–151, https://doi.org/10.1016/j.biopha.2017.02.003.

[26] V. Jain, N.K. Swarnakar, P.R. Mishra, A. Verma, A. Kaul, A.K. Mishra, N.K. Jain, Biomaterials Paclitaxel loaded PEGylated gleceryl monooleate based nanoparticulate carriers in chemotherapy, Biomaterials 33 (2012) 7206–7220, https://doi.org/10.1016/j.biomaterials.2012.06.056.

[27] L.O.F. Monteiro, R.S. Fernandes, L. Castro, D. Reis, G.D. Cassali, F. Evangelista, C. Loures, A.P. Sabino, V. Cardoso, C. Oliveira, A.B. De Barros, E.A. Leite, Paclitaxel-loaded folate-coated pH-Sensitive liposomes enhance cellular uptake and antitumor activity, Mol. Pharm. 16 (2019) 3477–3488, https://doi.org/10.1021/acs.molpharmaceut.9b00329.

[28] X. Zhang, Y. Huang, W. Zhao, Y. Chen, P. Zhang, J. Li, R. Venkataramanan, S. Li, PEG-farnesyl thiosalicylic acid telodendrimer micelles as an improved formulation for targeted delivery of paclitaxel, Mol. Pharm. 11 (2015) 2807–2814, https://doi.org/10.1021/mp500181x.

[29] M.I. Morais, F.F. Rodrigues, O.A.M. Costa, F.A. Goulart, C. Fábio, I.S.F. Melo, P.S.A. Augusto, M.G.B. Dutra, Â. De Fátima, M. Márcio, R.R. Machado, M.M.G.B. Dutra, Â. De Fátima, M.M. Coelho, R. Renes, Nicorandil inhibits mechanical allodynia induced by paclitaxel by activating opioidergic and serotonergic mechanisms, Eur. J. Pharmacol. 824 (2018) 108–114, https://doi.org/10.1016/j.ejphar.2018.02.014.

[30] C.M. De Souza, A.C. Araújo e Silva, C. De Jesus Ferraciolli, G.V. Moreira, L.C. Campos, D.C. Dos Reis, M.T.P. Lopes, M.ò.A.N.D. Ferreira, S.P. Andrade, G.D. Cassali, Combination therapy with carboplatin and thalidomide suppresses tumor growth and metastasis in 4T1 murine breast cancer model, Biomed. Pharmacother. 68 (2014) 51–57, https://doi.org/10.1016/j.biopha.2013.08.004.

[31] M.A. Dobrovolskaia, S.E. McNeil, Understanding the correlation between in vitro and in vivo immunotoxicity tests for nanomedicines, J. Control. Release 172 (2013) 456–466, https://doi.org/10.1016/j.jconrel.2013.05.025.

[32] Z. Zhang, L. Mei, S.-S. Feng, Paclitaxel drug delivery systems, Expert Opin. Drug Deliv. 10 (2013) 325–340, https://doi.org/10.1517/17425247.2013.752354.

[33] N. Desai, V. Trieu, Z. Yao, L. Louie, S. Ci, A. Yang, C. Tao, T. De, B. Beals, D. Dykes, P. Noker, R. Yao, E. Labao, M. Hawkins, P. Soon-shiong, Cancer Therapy : Preclinical Increased Antitumor Activity, Intratumor Paclitaxel Concentrations, and Endothelial Cell T ransport of Cremophor-Free, Albumin-Bound, Clin. Cancer Res. 12 (2006) 1317–1325, https://doi.org/10.1158/1078-0432.CCR-05-1634.

[34] W.J. Gradishar, Albumin-bound paclitaxel : a next-generation taxane, Expert Opin. Pharmacother. 7 (2006) 1041–1053, https://doi.org/10.1517/14656566.7.8.1041.

[35] J.V. Jokerst, T. Lobovkina, R.N. Zare, S.S. Gambhir, Nanoparticle PEGylation for imaging and therapy, Nanomedicine 6 (2011) 715–728, https://doi.org/10.2217/nnm.11.19.

[36] H. Maeda, Tumor-selective delivery of macromolecular drugs via the EPR effect: background and future prospects, Bioconjug. Chem. 21 (2010) 797–802, https://doi.org/10.1021/bc100070g.

[37] H. Chen, F. Wu, J. Li, X. Jiang, L. Cai, X. Li, DUP1 peptide modified micelle efficiently targeted delivery paclitaxel and enhance mitochondrial apoptosis on PSMA - negative prostate cancer cells, Springerplus. 5 (2016) 362, https://doi.org/10.1186/s40064-016-1992-0.

[38] L. Jiang, L. Li, X. He, Q. Yi, B. He, J. Cao, W. Pan, Z. Gu, Overcoming drug-resistant lung cancer by paclitaxel loaded dual-functional liposomes with mitochondria targeting and, Biomaterials. 52 (2015) 126–139, https://doi.org/10.1016/j.biomaterials.2015.02.004.

[39] A.M. Barbuti, Z. Chen, Paclitaxel through the ages of anticancer therapy : exploring its role in Chemoresistance and radiation therapy, Cancers (Basel). 7 (2015) 2360–2371, https://doi.org/10.3390/cancers7040897.

[40] D.R. Serrano, L. Hernández, L. Fleire, I. González-Alvarez, A. Montoya, M. P. Ballesteros, M.A. Dea-Ayuela, G. Miró, F. Bolás-Fernández, J.J. Torrado, Hemolytic and pharmacokinetic studies of liposomal and particulate amphotericin B formulations, Int. J. Pharm. 447 (2013) 38–46, https://doi.org/10.1016/j.ijpharm.2013.02.038.

[41] S.O. Rabah, Acute Taxol nephrotoxicity : histological and ultrastructural studies of mice kidney parenchyma, Saudi J. Biol. Sci. 17 (2010) 105–114, https://doi.org/10.1016/j.sjbs.2010.02.003.

[42] J.S. Baek, C.W. Cho, Controlled release and reversal of multidrug resistance by co-encapsulation of paclitaxel and verapamil in solid lipid nanoparticles, Int. J. Pharm. 478 (2015) 617–624, https://doi.org/10.1016/j.ijpharm.2014.12.018.

[43] Z. Li, S. Zhao, H. Zhang, P. Liu, F. Liu, Y. Guo, X. Wang, Proinflammatory factors mediate paclitaxel-induced impairment of learning and memory, Mediators Inflamm. (2018) (2018), 3941840, https://doi.org/10.1155/2018/3941840.

[44] M. Tsubaki, T. Takeda, M. Matsumoto, Tamoxifen suppresses paclitaxel-, neuropathy via inhibition of the protein kinase C / extracellular signal-regulated kinase pathway, J. Immunother. Emphasis Tumor Immunol. 40 (2018), https://doi.org/10.1177/1010428318808670, 1010428318808670.

[45] S.A. Dupre, D. Redelman, K.W. Hunter, The mouse mammary carcinoma 4T1 : characterization of the cellular landscape of primary tumours and metastatic tumour foci, Int. J. Exp. Pathol. 88 (2007) 351–360, https://doi.org/10.1111/j.1365-2613.2007.00539.x.

[46] G.H. Heppner, F.R. Miller, P.V.M. Shekhar, Nontransgenic models of breast cancer, Breast Cancer Res. 2 (2000) 331–334, https://doi.org/10.1186/bcr77.

[47] H.A. Blair, E.D. Deeks, Albumin-Bound Paclitaxel : A Review in Non-Small Cell Lung Cancer, Drugs. 75 (2017) 2017–2024, https://doi.org/10.1007/s40265-015-0484-9.